PHYSICAL CHARACTERIZATION OF 2020 AV$_2$, THE FIRST KNOWN ASTEROID ORBITING IN-SIDE VENUS' ORBIT.

M. Popescu[1], O. Vaduvescu[2,3], J. de León[3,4], C. de la Fuente Marcos[5], R. de la Fuente Marcos[6], J. Licandro[3,4], V. Pinter[3], O. Zamora[3,4], C. Fariña[2,3], L. Curelaru[7]; [1]Astronomical Institute of the Romanian Academy, 5 Cuţitul de Argint, 040557 Bucharest, Romania (mpopescu@aira.astro.ro), [2]Isaac Newton Group of Telescopes (ING), Apto. 321, 38700 Santa Cruz de la Palma, Canary Islands, Spain; [3]Instituto de Astrofísica de Canarias (IAC), C/Vía Láctea s/n, 38205 La Laguna, Tenerife, Spain; [4]Departamento de Astrofísica, Universidad de La Laguna, 38206 La Laguna, Tenerife, Spain; [5]Universidad Complutense de Madrid, Ciudad Universitaria, E-28040 Madrid, Spain; [6]AEGORA Research Group, Facultad de CC. Matemáticas, Universidad Complutense de Madrid, Spain; [7]Amateur Astronomer, Brasov, Romania;

Introduction: Numerical simulations predict the existence of a population of asteroids, which have their orbits entirely within Venus' orbit (Greenstreet et al. 2012). These objects that have values of the aphelion distance in the interval (0.307, 0.718) AU are called Vatiras. The first one, 2020 AV$_2$, has been discovered by the Zwicky Transient Facility on 4 January 2020 (Bacci et al. 2020). The latest orbit determination of this asteroid is characterized by an aphelion of 0.654 AU, a perihelion of 0.457 AU, and an orbital inclination of 16°.

In a recent paper, de la Fuente Marcos & de la Fuente Marcos (2020) reported that 2020 AV$_2$ appears to be a former Atira that entered the Vatira orbital domain about 10^5 yr ago. They showed that it displays an anti-coupled oscillation of the values of eccentricity and inclination, and that it might reach a 3:2 resonant orbit with Venus in the future, activating the von Zeipel–Lidov–Kozai mechanism. Similar conclusions have been independently reached by Greenstreet (2020).

The orbit of 2020 AV$_2$ makes it subjected to high temperature, strong solar wind irradiation, and close approaches to Mercury and (more distant) Venus. All these effects are transforming this minor body. Thus, its properties are a peculiar case compared with those of the near-Earth asteroids.

Observations and data reduction: We obtained spectroscopic and photometric data by using the 2.56m Nordic Optical Telescope (NOT) and 4.2m William Herschel Telescope (WHT), both located at El Roque de los Muchachos Observatory in La Palma, Canary Islands (Spain). The observations were made in difficult conditions due to the small solar elongation angle ~37° of 2020 AV$_2$. Thus, the object was observed at an altitude lower than 25° above the local horizon, and the data acquisition was started during the astronomical twilight. The observations were performed on the evenings of January 11, 13, and 14, 2020. We note that a better observing geometry can't be achieved using Earth-based telescopes.

Results: We obtained two visible spectra with ACAM/WHT and with ALFOSC/NOT instruments. The differences between them are within 1.7%,

smaller than the error bars. The near-infrared part of the spectrum was obtained with the LIRIS/WHT instrument using the *lr-zj prism*. It covers the 0.9-1.5 µm wavelength interval. In order to perform the analysis, the visible data obtained with ACAM/WHT (selected due to the smaller errors) was merged with the near-infrared one. The resulting spectrum is shown in Fig. 1.
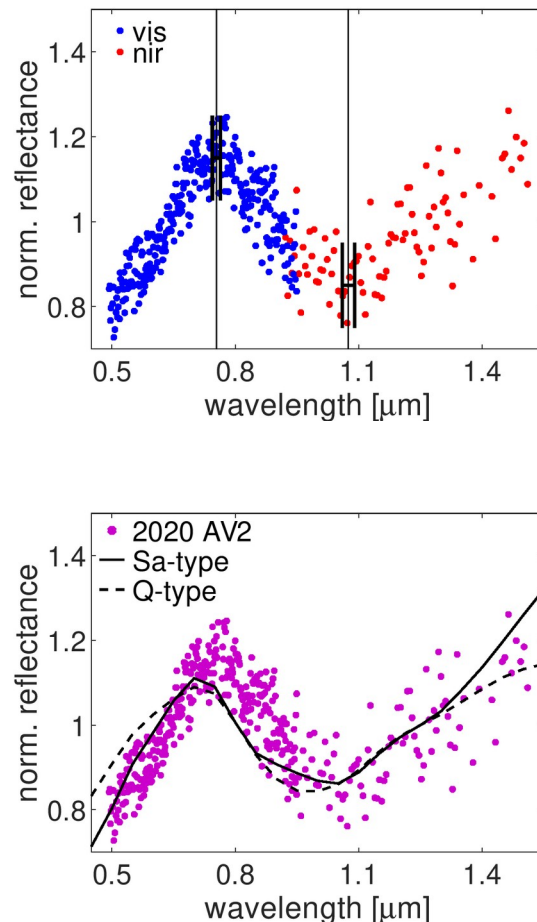

Figure 1. Spectral matching for 2020 AV$_2$. All spectra are The combined visible - near infrared spectrum is shown on the upper panel, normalized to unity at 1.25 µm.. The reflectance maximum at 0.745 µm and the band minimum at 1.075 µm are outlined by the

two markers. The comparison with the Sa-type and the Q-type is displayed in the lower panel.

The merged spectrum, covering a wavelength interval between 0.5-1.5 µm , shows a band minimum at *BImin* = 1.075 ± .015 µm. The *BImin* represents a rough approximation for the 1 µm band center (*BIC*), which is one of the main spectral features used to diagnostic the surface composition of asteroids. In order to compute the *BIC*, the continuum must be removed. We obtained an estimation of this by an extrapolation method coupled with a Monte-Carlo algorithm to estimate the error.

The value estimated for the *BIC* = 1.08 ± 0.020 µm points towards a composition similar to that of the S(I) subtype of asteroids with olivine-pyroxene mixtures, defined by Gaffey et al. (1993). These objects exhibit a strong 1 µm absorption feature, with a nonexistent or negligible 2 µm feature. The large value of the BIC is comparable only (at 2σ level) to the one shown by the olivine rich/dominated asteroids (Sanchez et al. 2014).

Following the equations shown by Sanchez et al. (2012), we determined the corrections due to temperature and phase angle effects. At the observing time, we estimate the subsolar equilibrium surface temperature as T = 350 K, and the object was observed at a phase angle of about 95°. These factors imply a wavelength correction ΔBIC = 0.003 µm for the band center, which is significantly less than our uncertainty σ_{BIC} = 0.020 µm, and can therefore be ignored. Thus, the *BIC* value is consistent with that of an object with an olivine-rich composition.

The visible spectral slope, computed over the 0.5 - 0.7 µm spectral interval, BR_{slope} = 17.7 ± 0.8%/0.1µm is intermediate between the slope of the S-complex and A-types. This parameter provides a way to quantify the reddening effects, which can be explained by phase angle, space-weathering, and grain size. The information currently available for this object doesn't allow disentangling these effects. Sanchez et al. (2012) found that the olivine-rich composition shows the largest variation of spectral slope with increasing phase angle. However, their slopes were computed over the entire 0.45 - 2.5 µm spectral interval. The slope we determined for 2020 AV_2 is comparable to those found by Perna et al. (2018) for the S-type asteroids observed at about 90° phase angle.

The taxonomic classes that best fit the spectrum of 2020 AV_2 are Sa, A, and Q-type. The match was computed by using the least squared differences. The main feature that weights the result is the broad 1 µm band. The center of this band is most similar to those of the Sa, and A-type. We favor a Sa type classification, which is an intermediate class between S-complex and A-types.

The average albedo for the S-complex asteroids is p_V = 0.22 ± 0.07, (Mainzer et al. 2011). For an absolute magnitude of H=16.4 ± 0.77 mag (JPL Small-Body Database Browser, accessed on 22/02/2020), we can constrain its equivalent diameter to $1.5^{+1.1}_{-0.6}$ km.

The images obtained with the J and K_s filters, during the LIRIS/WHT observations show a stellar profile with a median full width at half maximum of 1.5 arcsec, which is equal to that of the stars.

In order to extend the data arc and improve the orbit determination, we performed a data-mining of world-wide astronomical archives using EURONEAR MegaPrecovery software (reference to this software). However, we were not able to find any observations acquired prior to its discovery.

References: [1] Greenstreet, S. et al.; Icarus, 217, 1, p. 355-366 (01/2012); [2] Bacci P. et al.; MPEC 2020-A99 (01/2020); [3] Gaffey, M. J. et al.; Icarus, 106, 2, p. 573-602 (12/1993); [4] Sanchez, J. A. et al.; Icarus, 228, p. 288-300 (01/2014); [5] Sanchez, J. A. et al.; Icarus, 220, 1, p. 36-50 (07/2012); [6] Perna, D. et al.; PSS, 157, p. 82-95 (08/2018); [7] de la Fuente Marcos, C., de la Fuente Marcos, R.; Accepted for publication in MNRAS (02/2020); [8] Mainzer A. et al.; AJ, 741, 2,id. 90 (11/2011); [9] Vaduvescu, et al.; Astronomy and Computing, 30 (01/2020); [10] Greenstreet; MNRAS, 493, (03/2020).